Composition of the continuous phase in partially miscible blends of epoxy resin and epoxidized rubber by dynamic mechanical analysis

Philippe Bussi and Hatsuo Ishida*
Department of Macromolecular Science, Case Western Reserve University, Cleveland, OH 44106, USA
(Received 29 March 1993)

The dynamic mechanical properties of blends of diglycidyl ether of bisphenol-A based epoxy resin and internally epoxidized polybutadiene rubber have been studied as a function of initial rubber content, stoichiometry and cure cycle of the epoxy resin. It is shown that both the glass transition temperature of the epoxy-rich continuous phase, $T_{\mathrm{gE(r)}}$, and the apparent enthalpy of activation associated with this transition, $\Delta H_{\mathrm{a_{E(r)}}}$, are sensitive to the state of the rubber in the sample. Specifically, dynamic mechanical analysis can be used to distinguish between rubber dissolved in the matrix (plasticizer), incorporated into the network (flexibilizer) or phase separated (toughener). Furthermore, it is demonstrated that the Gordon–Taylor equation rather than the more commonly used Fox equation should be used to model the effect of dissolved rubber on $T_{\mathrm{gE(r)}}$ and that the Gordon–Taylor equation can also be extended to describe the variations of $\Delta H_{\mathrm{a_{E(r)}}}$. Ultimately this equation can be generalized to predict the glass transition temperature of a sample containing both dissolved and phase separated rubber.

(Keywords: composition; blends; dynamic mechanical analysis)

INTRODUCTION

Low levels of rubber are routinely added to epoxy formulations to tailor the properties of these systems. It is well-known that a small amount of a reactive rubber can greatly improve the fracture toughness of epoxy resins by forming discrete rubbery particles that are chemically bonded to the matrix[1]. The toughening effect is generally accompanied by a relatively small loss of thermomechanical properties. Non-reactive, compatible rubber is also used as a plasticizer to increase the ductility of epoxy resins while preserving the transparency. Both chemistry and thermodynamics play an essential role in determining the final properties of these rubber/epoxy blends. Indeed the balance between phase separation and polymerization determines whether dilution, phase separation or even phase inversion occurs. It also dictates the composition of each phase, the volume fraction of dispersed rubber, the particle size and particle size distribution and the degree of interaction between phases. This balance is most affected by the degree of compatibility between the rubber and the epoxy, the amount of rubber present in the sample and the epoxy resin curing cycle.

Dissolved rubber and phase separated rubber are expected to modify the physical and mechanical properties of these blends in a complementary manner. Recent work[2,3] has shown that plastic shear yielding in the matrix is the main source of increased toughness. The presence of rubbery particles creates stress concentrations which act as initiation sites for the plastic shear deformation of the matrix. Cavitation of the rubbery particles provides an additional dissipation mechanism. On the other hand, dissolved rubber increases matrix ductility and reduces the level of stress at which shear bands initiate. Thus it becomes important to properly characterize these multiphase systems. However this task can be difficult. Indeed the epoxy matrix can accommodate the rubber in three different ways: composition of the continuous phase, composition of the dispersed phase; and volume fraction of dispersed phase. The situation is summarized by the following equation, derived from a mass balance:

$$\Phi_{\mathrm{R}}^{0}=(1-V_{\mathrm{D}})\Phi_{\mathrm{R}}^{\mathrm{C}}+V_{\mathrm{D}}\Phi_{\mathrm{R}}^{\mathrm{D}} \qquad (1)$$

where Φ_{R}^{0} is the initial volume fraction of rubber introduced in the matrix, $\Phi_{\mathrm{R}}^{\mathrm{C}}$ is the composition of the continuous phase, $\Phi_{\mathrm{R}}^{\mathrm{D}}$ that of the dispersed phase, and V_{D} is the volume fraction of the dispersed phase. The complexity of the problem comes from having one known input (Φ_{R}^{0}) but three unknown variables ($\Phi_{\mathrm{R}}^{\mathrm{C}}$, $\Phi_{\mathrm{R}}^{\mathrm{D}}$, V_{D}) for just one equation. For practical purposes, $\Phi_{\mathrm{R}}^{\mathrm{C}}$ and V_{D} are the most important parameters.

The primary goal of this paper is to show how dynamic mechanical analysis (d.m.a.) can be used to describe both qualitatively and quantitatively the complex behaviour of rubber/epoxy blends. While most commercial systems rely on a carboxylic acid terminated butadiene acrylonitrile copolymer (CTBN), this study utilizes an epoxidized, hydroxyl terminated polybutadiene rubber (E-HTB). In this paper, a very

---

* To whom correspondence should be addressed

0032-3861/94/05/0956-11

compatible grade (high oxirane content) has been used in order to magnify the effect of dissolved rubber. The influence of rubber content, stoichiometry and cure temperature of the epoxy resin is investigated. In a subsequent paper[4], a less compatible grade has been used in order to study more specifically how the volume fraction of dispersed phase can be evaluated by d.m.a.

EXPERIMENTAL

Materials

The epoxy system used in this study was a diglycidyl ether of bisphenol-A (DGEBA) epoxy resin cured with bisphenol-A and catalysed by a tertiary amine (Lewis base). Depending on the reaction conditions and on the initial stoichiometry, this versatile material can exhibit a thermoset or thermoplastic character[5]. The crosslink density and the degree of branching can be controlled to promote either stiffness or toughness. An excess of bisphenol-A favours growth of the chains whereas excess diepoxide promotes branching and crosslinking. This system is commonly employed in industry with a bisphenol-A to DGEBA stoichiometric ratio, s, of 0.6. Bisphenol-A is often used in rubber toughening applications because it seems to enhance the toughening effect of the rubber[1,2,6,7]. In a non-toughened system, it is used primarily as a chain extender. The glass transition temperature, T_g, of the cured epoxy is ~100–103°C. The DGEBA resin, Epon 828, and the bisphenol-A were obtained from Shell Chemical Corporation. The catalyst, *p*-chlorophenyl-1,1-dimethylurea (trade name Monuron) is manufactured by DuPont.

Three different grades of E-HTB resins were available for this study. The internal oxirane groups present on the polybutadiene backbone are obtained by reaction of *cis* and *trans* unsaturations with an organic peracid. The microstructure characterization as well as the reactivity of these resins has been reported previously[8]. It was shown that: (1) the formation of rubber/epoxy adduct during polymerization through the terminal hydroxyl end groups is unlikely unless special precautions such as pre-reaction of the rubber are taken; and (2) matrix gelation occurs long before substantial reaction of the internal oxirane groups with bisphenol-A can take place. These resins (trade name Poly bd) were provided by Elf Atochem. They have the following structure:

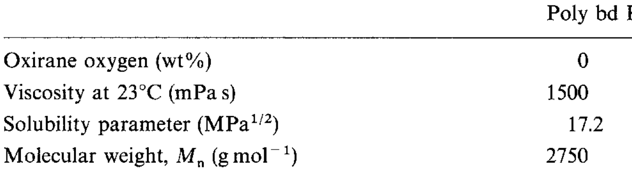

and some of their properties are presented in *Table 1*. Poly bd 600 and Poly bd 605 are hereafter described as low-epoxidized and medium-epoxidized rubber, respectively. All materials in this study were used as received without further purification. However, bisphenol-A was dried at 110°C for 12 h prior to use, as water content can influence the kinetics of the diepoxide/bisphenol-A reaction.

When the rubbers are mixed with the uncured epoxy resin, the result depends on the degree of epoxidation and the mixing temperature. A mixture of the medium-epoxidized rubber with the DGEBA resin is clear at room temperature in the range of rubber content investigated. On the other hand, a similar mixture using the low-epoxidized rubber is milky in appearance at room temperature but becomes clearer after stirring at typical moulding temperatures. In cured samples, phase separation depends on both the rubber content and the stoichiometric ratio selected for the epoxy matrix. As a rule, the amount of rubber that can be dissolved in the matrix without phase separation increases with the stoichiometric ratio. As the stoichiometric ratio increases, the epoxy network becomes looser and more of the rubber can be accommodated. With an excess of bisphenol-A ($s > 1$) it is possible to avoid phase separation in a cured sample with as much as 40 wt% of the medium-epoxidized rubber. In this case, a blend of a linear thermoplastic epoxy with an epoxidized rubber is obtained.

Sample preparation and apparatus

Sample preparation. Epoxy resin/epoxidized rubber samples are prepared in the following typical manner. The catalyst (2% of total weight of the mixture) is added as a finely ground powder to the diepoxide preheated at 80°C. The mixture is stirred for ~5 min to ensure proper dispersion of the catalyst. The epoxidized rubber and the diepoxide are degassed separately in a vacuum oven at 80°C for 20 min. The rubber is then mixed with the diepoxide and the resulting homogeneous mixture is stirred for 5 min before being degassed for 20 min at 80°C. Meanwhile, bisphenol-A is molten in a separate oven at 160–170°C. It is then quickly added to the rubber/diepoxide mixture and stirred vigorously for 15 s. The content of the beaker is then poured into a preheated, levelled, aluminium mould. Typical cure cycle times are 7 h at 100°C followed by an immediate post cure at 125°C for 4 h. At 100°C and for $s = 1$, gelation occurs[5] after ~60 min. The samples are then slowly cooled to room temperature to avoid excessive warpage. Sample

Table 1 Physico-chemical properties of the E-HTB resins used in this study

	Poly bd R20LM	Poly bd 600	Poly bd 605
Oxirane oxygen (wt%)	0	3.5	6.1
Viscosity at 23°C (mPa s)	1500	5500	23 000
Solubility parameter (MPa$^{1/2}$)	17.2	17.7	18.2
Molecular weight, M_n (g mol^{-1})	2750	2940	3270
Polydispersity	2.3	2.4	2.8
Specific gravity at 23°C	0.90	1.01	1.01
Glass transition temperature, T_g (°C)	−75	−60	−47

nomenclature follows these guidelines:

	M/*s*06/16/100
First sequence	rubber type [low-epoxidized (L), medium-epoxidized (M)]
Second sequence	stoichiometric ratio *s* (0.3 or 0.6)
Third sequence	rubber content (in parts per hundred parts epoxy resin, phr)
Fourth sequence	Pre-cure temperature (80, 100 or 150°C)

Rubber content is ultimately expressed in terms of the weight fraction of rubber, w_R.

Dynamic mechanical analysis (d.m.a.). Dynamic mechanical spectra were obtained on a Rheometrics dynamic mechanical spectrometer RMS-800 with a temperature capability ranging from -150 to 600°C. A force rebalanced transducer with 2000 g cm torque was used with a rectangular sample torsion fixture. Measurements were made at 2°C intervals at a rate of $2°C\,min^{-1}$. The transition temperatures reported for the observed relaxations are obtained from the maxima in the loss spectrum (loss modulus, G'', *versus* temperature), unless otherwise specified. Frequency/temperature sweeps were conducted in order to determine the apparent enthalpy of activation of the epoxy α transition (frequency range 1–$100\,rad\,s^{-1}$, temperature range 25–150°C). Lower frequencies (0.1–$10\,rad\,s^{-1}$) were used to resolve the low temperature region (-110 to -40°C) where the α transition of the rubber and β transition of the epoxy resin overlap.

Scanning electron microscopy (SEM). Fracture surfaces of rubber/epoxy blends were studied with a Joel JSM-35CF scanning electron microscope, after coating the samples with a thin layer of gold. The samples were fractured at room temperature in a single edge notch (SEN) test, at a cross-head speed of $1\,mm\,min^{-1}$. Verchere *et al.*[9] have recently indicated that morphological parameters determined by SEM are not affected by the type of fracture mode (mechanical solicitation and strain rate). Statistical analysis was conducted on magnified micrographs, where at least 150 particles and up to 300 particles were considered for each composition. The particle size distribution and the average number of particles per unit area, $\bar{N}$ (particles μm^{-2}), were obtained. The number average particle diameter, $\bar{D}$ (SEM), is then calculated as:

$$\bar{D}(\mathrm{SEM})=\frac{\sum_i n_i D_i}{\sum_i n_i} \qquad (2)$$

The volume fraction of dispersed phase, V_D (SEM), is expressed as:

$$V_D(\mathrm{SEM})=\left(\frac{\pi}{4}\right)\frac{\sum_i n_i D_i^2}{A_{\mathrm{ref.}}} \qquad (3)$$

where $A_{\mathrm{ref.}}$ is the reference area under observation. Both Butta *et al.*[10] and Verchere *et al.*[9] have discussed the validity of a direct determination of V_D from SEM observations. In particular, Verchere *et al.* pointed out that the more commonly used method of determination by transmission electron microscopy only gives an apparent value of V_D and that SEM measurements are preferred.

RESULTS AND DISCUSSION

Scanning electron microscopy

Influence of the rubber content and of the epoxy resin stoichiometric ratio. The fracture surface of the pure epoxy resin is shown in *Figure 1* and can be compared with the typical morphology for M/*s*06/100 samples (*Figure 2*). There is a significant increase in roughness between the fracture surface of the pure resin and that of the blend. This phenomenon is indicative of increased shear deformation. The apparent holes in *Figure 2* correspond to the cavitation of rubbery particles. That these holes are indeed filled with rubber can be shown either by using a higher magnification or by letting the rubber particles swell out of the cavities after exposure to solvent[3,10]. Cavitation (voiding) is also the reason for the observed macroscopic stress whitening. The medium-epoxidized rubber is very compatible with the epoxy resin selected. Thus a significant weight fraction of rubber, ~6%, must be added before optical clarity is lost. Optical clarity indicates either total dissolution of the rubber or absence of particles above a critical size (~0.15 μm). Observation of the fracture surface for the clear blends reveals that rubbery particles are indeed present but are of small diameters (0.1–0.2 μm). Thus optical clarity is preserved.

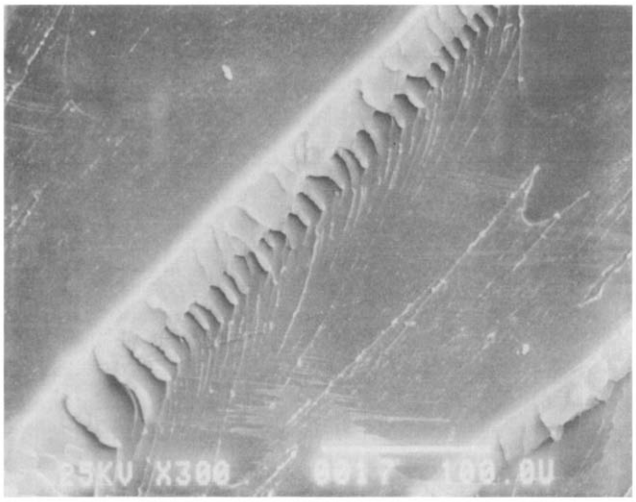

Figure 1 Fracture of the pure epoxy sample, near the crack tip

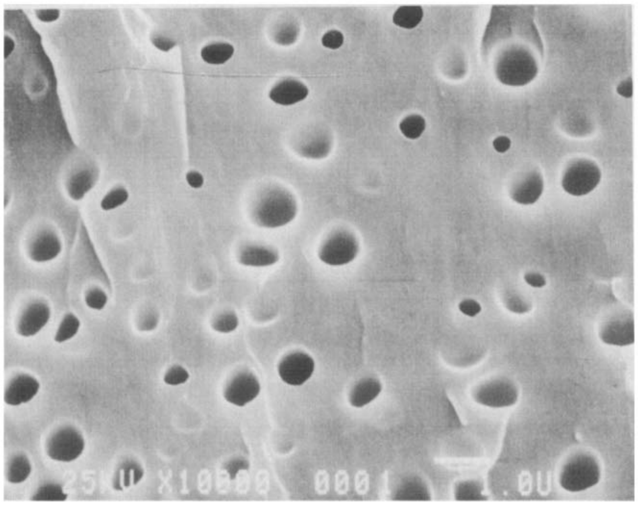

Figure 2 Fracture surface of a typical epoxidized rubber/epoxy resin blend (M/*s*06/24/100 sample), in the stress-whitened region

For practical applications it is often desirable to control both the average diameter of the rubber particles, $\bar{D}$, and the volume fraction of the dispersed phase, V_D. One way to affect these parameters is to modify the matrix network structure. By increasing the DGEBA content of the epoxy resin (M/*s*03/100 samples), a tighter epoxy network is created. Whereas the polymerization kinetics are not drastically affected by such a change, the tighter network changes the phase separation behaviour. Indeed optical clarity is now lost at lower rubber content, ~4%. The effect of stoichiometry on both $\bar{D}$ and V_D is illustrated in *Figures 3* and *4*. The size of the rubbery particles increases regularly with rubber content for both cases. The initial increase is sharper for M/*s*03/100 samples and reflects the larger driving force toward phase separation. Eventually $\bar{D}$ levels off to ~0.85 μm. By contrast, D increases more slowly for M/*s*06/100 samples to ~0.65 μm. The volume fraction is very low before phase separation occurs but increases continuously afterwards. However, even at ~15% of rubber, V_D remains quite low (~0.11). It is worth noting that the change in matrix network structure has almost no effect on the amount of dispersed phase. The volume fraction starts to increase in both cases at ~4% added rubber. This indicates that the later loss of optical clarity observed with M/*s*06/100 samples at 6% rubber content is solely due to the fact that these samples contain smaller particles. Last, a corollary to *Figures 3* and *4* is that the concentration of particles is larger for the looser matrix ($\bar{N}_{M/s06/100} \cong 0.9$ particle μm^{-2} *versus* $\bar{N}_{M/s03/100} \cong 0.2$ particle μm^{-2}).

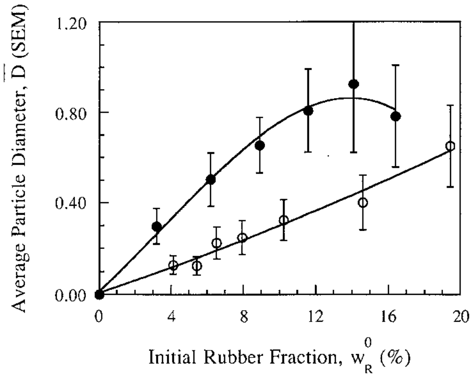

Figure 3 Effect of rubber content, w_R^0, and stoichiometry on the average particle diameter, $\bar{D}$: (●) M/*s*03/100; (○) M/*s*06/100

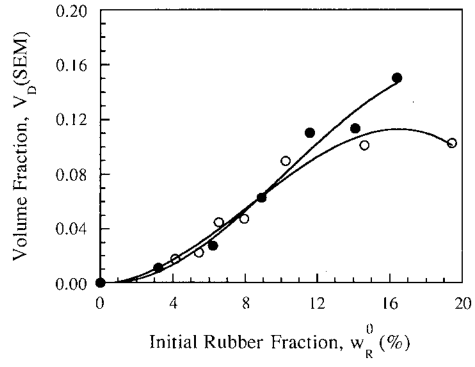

Figure 4 Effect of rubber content, w_R^0, and stoichiometry on the volume fraction of dispersed phase, V_D: (●) M/*s*03/100; (○) M/*s*06/100

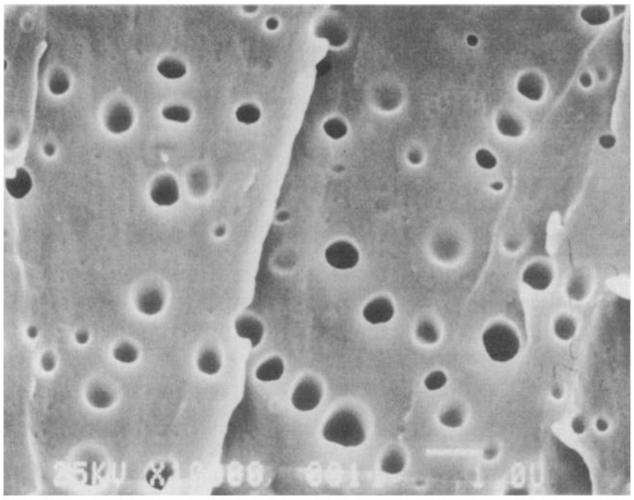

Figure 5 Fracture surface of a typical epoxidized rubber/epoxy resin blend containing 14.7% rubber (M/*s*06/24/80 sample), in the stress-whitened region

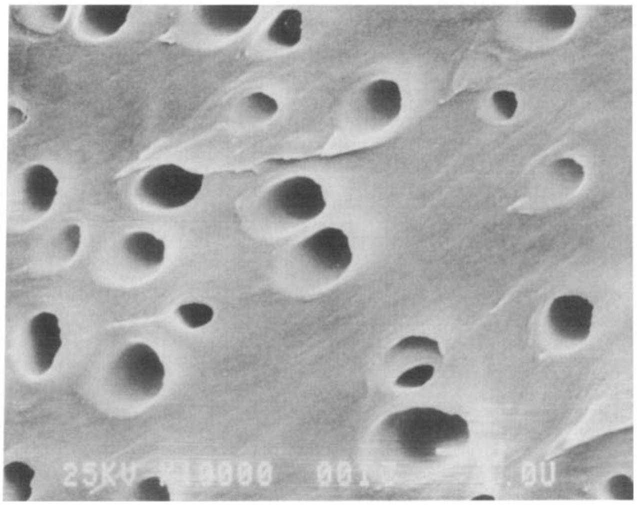

Figure 6 Fracture surface of a typical epoxidized rubber/epoxy resin blend containing 14.7% rubber (M/*s*06/24/150 sample), in the stress-whitened region

Influence of the epoxy cure temperature. So far, it has been shown that rubber content has a strong influence on both $\bar{D}$ and V_D while the epoxy resin stoichiometric ratio controls more specifically $\bar{N}$ and $\bar{D}$ by altering the balance between phase separation and polymerization. The influence of the epoxy curing temperature is now discussed. In rubber/epoxy blends, phase separation of the rubber is generally much faster than polymerization of the epoxy resin[11]. Also, cure temperature affects the polymerization rate much more than the phase separation rate. At a low cure temperature, the local viscosity is rising slowly so that the rubber has ample time to phase separate. Consequently, the amount of rubber dissolved in the epoxy matrix is low. By contrast, a high cure temperature results in fast gelation and more of the rubber is trapped into the matrix before it has a chance to fully phase separate. In order to study this effect, M/*s*06 samples containing 14.7% of rubber were moulded at 150°C for 4 h and at 80°C for 24 h. The M/*s*06/80 sample was also post-cured at 125°C for 4 h so that the results could be compared with M/*s*06/100 samples. Typical fracture surfaces for these samples are shown in *Figures 5* and *6*. As expected, the sample cured at 150°C (*Figure 6*) exhibits less phase separation than the sample cured at 80°C (*Figure 5*). However the average particle diameter is larger. One of the limitations of SEM is that it does not yield any information about the amount of dissolved rubber in the continuous phase. It will now be shown that d.m.a. is particularly adapted to this kind of task.

Dynamic mechanical analysis

D.m.a. is one of the few techniques that enables one to selectively look at the different components of a multiphase system and their interactions. This is illustrated in *Figure 7* where selected features of the spectrum of a typical blend are correlated with specific regions in the phase separated sample. The features of interest are: (1) the glass transition region of the epoxy resin, where the continuous epoxy phase containing a small amount of rubber, E(r), is probed; (2) the glass transition region of the rubber, which characterizes the rubber-rich domains containing a small amount of epoxy resin, R(e). This region overlaps with the epoxy resin β transition region, also related to E(r); (3) the shape of the spectrum in the epoxy glass transition region, and (4) the plateau region where the level of elastic modulus, G', can be related to the epoxy network structure and to the volume fraction of dispersed phase. Features (1) and (2) will now be discussed in more detail, as the influence of rubber content, stoichiometric ratio and cure temperature is also examined. The shape of the spectrum (3) and the rubbery plateau region (4) are examined elsewhere[4,12].

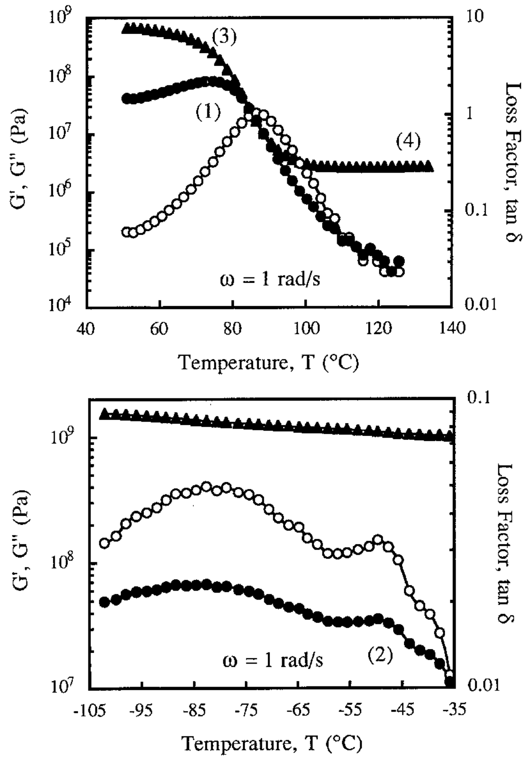

Figure 7 D.m.a. spectrum of M/s06/28/80 sample. Features of interest are: (1) the glass transition region of the epoxy resin (continuous phase); (2) the glass transition region of the rubber (dispersed phase); (3) the shape of the spectrum in the transition region; and (4) the rubbery plateau region. (▲) Elastic modulus, G'; (●) loss modulus, G''; and (○) loss factor, tan δ

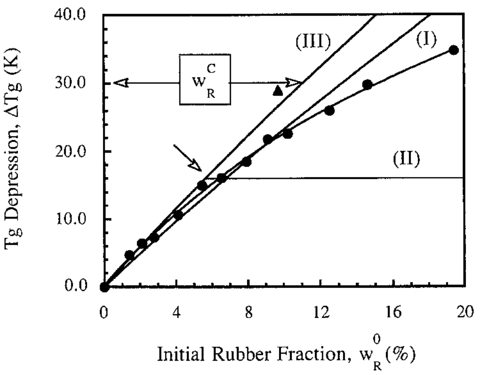

Figure 8 Depression of the epoxy glass transition temperature, $\Delta T_{gE(r)}$, as a function of rubber content, w_R^0 [M/s06/100 samples, (●)]. (I) Total dissolution behaviour, as modelled by the Fox equation. (II) Ideal phase separation behaviour. (III) Total dissolution behaviour, as modelled by the Gordon–Taylor equation. (▲) ΔT_g in a sample for which the rubber acts as a flexibilizer rather than as a plasticizer (see text)

Epoxy resin glass transition region. (1) Influence of the rubber content and of the epoxy resin stoichiometric ratio. The position of the epoxy resin glass transition temperature, $T_{g_{E(r)}}$, is a good indicator of the amount of rubber dissolved in the matrix. Dissolved rubber facilitates the co-operative movement of the epoxy segments in the network. Thus $T_{g_{E(r)}}$ is depressed by an amount $\Delta T_g = T_{g_{E(0)}} - T_{g_{E(r)}}$, where $T_{g_{E(0)}}$ is the glass transition temperature of the pure epoxy resin. *Figure 8* is a plot of ΔT_g as a function of rubber content for M/s06/100 samples. A significant amount of dissolved rubber is expected since V_D is low in these samples (*Figure 4*). Indeed, this grade of epoxidized rubber appears very compatible with the epoxy matrix as evidenced by the large values of ΔT_g (30K at 15 wt% rubber). Clearly a diluent effect is seen. Two equations, the Fox equation[13] and the Gordon–Taylor equation[14], are generally used to evaluate the weight fraction of dissolved rubber, w_R^C. Their relative usefulness is now discussed. In *Figure 8*, line (I) represents the predicted ΔT_g from the Fox copolymer equation:

$$\frac{1}{T_{g_{E(r)}}} = \frac{w_E^C}{T_{g_{E(0)}}} + \frac{w_R^C}{T_{g_{R(0)}}} \tag{4}$$

where $T_{g_{E(0)}}$ and $T_{g_{R(0)}}$ are the glass transition temperatures of the unplasticized epoxy and pure rubber and w_E^C and w_R^C are the corresponding weight fractions ($w_R^C = 1 - w_E^C$). Thus:

$$\Delta T_{g_{Fox}} = \frac{w_R^C T_{g_{E(0)}}(T_{g_{E(0)}} - T_{g_{R(0)}})}{w_R^C(T_{g_{E(0)}} - T_{g_{R(0)}}) + T_{g_{R(0)}}} \tag{5}$$

The Fox equation models the total dissolution behaviour, that is when all of the rubber initially added is dissolved into the epoxy continuous phase. This simple equation fits the first few data points reasonably well. Notice that there are no adjustable parameters in equation (5) since $T_{g_{E(0)}}$ and $T_{g_{R(0)}}$ as well as w_R^C are known [$T_{g_{E(0)}} = 376$K and $T_{g_{R(0)}} = 226$K as determined in this study (see Appendix)]. There are two problems with equation (5). First, it underestimates the experimental dissolution effect at low rubber content. As a result, a crossover point is observed at ~10%. This is especially a problem because the experimental ΔT_gs are already lower than the theoretical maximum corresponding to true total dissolution. Indeed, even at low rubber content, there is always a small but non-zero volume fraction of dispersed phase as shown in the SEM study (*Figure 4*). Therefore, if anything, the model [line (I)] should be the envelope of the experimental data. Second, the Fox equation does not recognize properly the onset of phase separation. Previously, this event was defined as the loss of optical clarity and occurred at ~6%. In *Figure 8*, a significant deviation from the predicted ΔT_gs does not occur until ~12% rubber content is reached. The Fox equation interprets the system as more plasticized than it truly is. Two possible sources for this discrepancy are discussed in the following section.

First, it should be recognized that after the limit of total dissolution has been reached ($w_R^0 = 0.06$, $\Delta T_g = 16$K), one would expect ΔT_g to remain constant because the epoxy matrix has accommodated all the rubber it can at that point. Thus any amount of rubber that is further introduced should now contribute entirely to the formation of a dispersed phase. The experimental curve lies between the total dissolution line (whether modelled by the Fox equation or the Gordon–Taylor equation) and the ideal phase separation line (II). This indicates that dissolution still occurs after the onset of phase separation although the increase in ΔT_g with w_R^0 is now less marked. The non-ideality arises because polydispersity is neglected in this interpretation. Phase separation in high polymers depends on molecular weight. Thus, a high molecular weight fraction might phase separate while the corresponding low molecular weight material remains in solution, thereby further lowering $T_{g_{E(r)}}$. In applying equation (5), the effect of molecular weight segregation on the value of $T_{g_{R(0)}}$ has been neglected. Since the starting epoxidized rubber already has a low molecular weight ($M_n = 3270\ \mathrm{g\,mol^{-1}}$), additional segregation can result in a substantial lowering of the real $T_{g_{R(0)}}$, possibly by as much as 10K as documented by Boyer[15]. A lower $T_{g_{R(0)}}$ would in turn result in an increase of ΔT_g as predicted by the Fox equation.

Second, the Fox equation is a particular case of the more general Gordon–Taylor equation[14]. The two equations are equivalent only under particular conditions that are not met in the present case. The Gordon–Taylor equation predicts the T_g of binary copolymers from the T_gs of the pure polymers, the weight fraction of each component and the thermal expansion coefficients in the glassy and rubbery states. The copolymer chain is treated as a mixture of small molecules for which the ideal volume additivity law is assumed to hold. A similar simplifying assumption can be made in the case of a plasticized epoxy network, i.e. the total free volume of the system is a weighted sum of the free volume of each component. Following the original paper:

$$w_R^C = \frac{T_{g_{E(0)}} - T_{g_{E(r)}}}{[k(T_{g_{E(r)}} - T_{g_{R(0)}}) + (T_{g_{E(0)}} - T_{g_{E(r)}})]} \tag{6}$$

So that:

$$\Delta T_{g_{GT}} = \frac{k w_R^C (T_{g_{E(0)}} - T_{g_{R(0)}})}{1 + w_R^C (k-1)} \tag{7}$$

k is a constant defined as:

$$k = \frac{({}_2\beta_R - {}_2\beta_G)}{({}_1\beta_R - {}_1\beta_G)} = \frac{\Delta_2\beta}{\Delta_1\beta} \tag{8}$$

where β is the first derivative of the specific volume, V ($V = 1/\rho$, ρ is the density), with respect to temperature and R and G refer to the rubbery and glassy state, respectively. Here, component 1 is the epoxy resin while component 2 is the epoxidized rubber. β is closely related (by a factor $1/V$) to the coefficient of thermal expansion, α [$\alpha = (\partial V/\partial T)_P/V$]. $\Delta\beta$ represents the jump in β at the glass transition and is related to the more commonly used quantity $\Delta\alpha$:

$$\Delta\beta = V_{(T=T_g)}\Delta\alpha = \Delta\alpha/\rho_{(T=T_g)} \tag{9}$$

Equation (7) and equation (5) are equivalent (i.e. $\Delta T_{g_{GT}} = \Delta T_{g_{Fox}}$) only if k has the following specific value, k_0:

$$k_0 = \frac{T_{g_{E(0)}}}{T_{g_{R(0)}}} \tag{10}$$

The significance of this special case is made clearer if one assumes that both components 1 and 2 follow the Simha–Boyer relationship, reviewed in Boyer[15]:

$$\Delta\alpha_i T_{g_i} \cong 0.113 \tag{11}$$

Combining equations (8), (9), (10) and (11):

$$k = \frac{V_2\Delta\alpha_2}{V_1\Delta\alpha_1} \cong \frac{\rho_1}{\rho_2} k_0 \tag{12}$$

Equation (12) states that the Fox equation and the Gordon–Taylor equation are equivalent ($k = k_0$) only if the two materials have a similar density at their respective T_gs. Clearly this is not the case for a polybutadiene rubber and an epoxy resin. Thus the Fox equation should not be expected to apply. For the polybutadiene/epoxy pair, equation (12) indicates that $\Delta T_{g_{GT}} > \Delta T_{g_{Fox}}$. One can crudely estimate $k = 2.0$ using the room temperature value of the density for the polybutadiene and the epoxy resin. Practically, k can be obtained from the best possible fit of the experimental ΔT_gs for optically clear samples [line (III) in *Figure 8*]. One finds $k_{\text{best fit}} = 1.95$, in good agreement with the estimated value. Deviation from the predicted ΔT_gs signals the onset of phase separation. This deviation is observed at ~6% and correlates well with visual inspection. The constant k can also be estimated more rigorously from equation (8) without using the simplifying assumption of the Simha–Boyer relationship. From literature[14,16], $\Delta\beta_{\text{Poly bd}} \cong 6.6 \times 10^{-4}\ \mathrm{g\,cm^{-3}\,K^{-1}}$ and $\Delta\beta_{\text{epoxy}} \cong 3.0 \times 10^{-4}\ \mathrm{g\,cm^{-3}\,K^{-1}}$, which yields $k \cong 2.20$, close to the experimental value. In *Figure 8* a special data point (▲) has also been added. This data point was obtained for a M/*s*06/15/100 sample containing 9.7% of the medium-epoxidized rubber which had been pre-reacted with excess diepoxide (3 h at 113°C). This functionalized medium-epoxidized rubber becomes extremely soluble. It also shows more reactivity with the epoxy matrix. Thus, upon curing, the rubber is incorporated into the epoxy network and acts as a flexibilizer instead of a plasticizer. As a result there is virtually no phase separation. This sample exhibits a ΔT_g of ~30K which is 9K higher than the corresponding sample containing the non-pre-reacted rubber. This value of 30K is extremely close to the value predicted from the Gordon–Taylor equation. Therefore, this is a good indication that line (III) in *Figure 8* does indeed represent the total dissolution behaviour.

So far, the epoxy resin glass transition region has been characterized by a single parameter, ΔT_g. However, the position of the glass transition, as well as other relaxations, also depend on test frequency. At higher frequencies, the glass transition shifts to higher temperatures as illustrated on a relaxation map for different sample compositions (*Figure 9*). As an example, $T_{g_{E(r)}}$ for a sample containing 19.4% rubber increases by

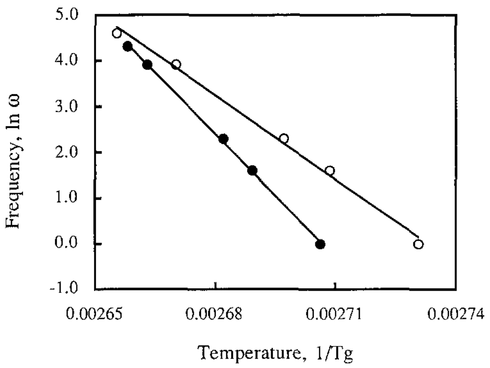

Figure 9 Relaxation map for M/*s*06/100 samples containing 2.1% rubber (●) and 19.4% rubber (○). The abscissa for the M/*s*06/34/100 data (○) has been shifted for clarity by −0.0002 units

9K from a base value of 68°C when the test frequency changes from 1 to 100 rad s^{-1}. To illustrate the practical importance of test frequency, or time-scale, consider the case of toughness measurements by two different test methods, single edge notch (SEN) or impact test (IZOD). If one assumes[17] that the frequency corresponding to a SEN test is about ~1 Hz whereas that for an IZOD test is ~1000 Hz, the corresponding increase in T_g is ~17 K. It is clear that, based on time-scale considerations alone, these two tests conducted at the same temperature, on the same sample, are in fact measuring toughness of a sample in two different physical states. Most recently, the work of Kinloch and Hunston[3,18] has shown that the concept of time/temperature superposition can be applied to fracture energy measurements.

From *Figure 9*, one can calculate an *apparent* enthalpy of activation for the epoxy resin glass transition, ΔH_a, assuming that Arrhenius behaviour is followed. The word *apparent* should be emphasized here as the glass transition is not entirely a thermodynamic process (T_g is not a true second-order transition) but also a kinetic process. Therefore an Arrhenius behaviour is not expected to apply. The work of Williams *et al.*[19] has shown that a true ΔH_a is a function of temperature around T_g. This temperature dependency accounts for the curvature sometimes observed in relaxation plots (Arrhenius plots). However *Figure 9* shows that in the present case an Arrhenius behaviour describes the data resonably well for the frequency range investigated even though a slight curvature is observed. Therefore $\Delta H_{a_{\mathrm{Arrhenius}}}$ was selected because it is a convenient way to describe the frequency dependency of $T_{g_{E(r)}}$. The use of $\Delta H_{a_{\mathrm{Arrhenius}}}$ is also appropriate in this study since one is more interested in the variations of ΔH_a with different parameters than in its absolute magnitude. Finally, values of $\Delta H_a/R$ (in K), where R is the gas constant, rather than of ΔH_a (in kcal mol^{-1}) are reported in this study because the exact meaning of a mole of moving units involved in the glass transition is difficult to define.

Figure 10 is a plot of $\Delta H_a/R$ as a function of rubber content for M/*s*06/100 samples. The initial value for the pure epoxy, $\Delta H_a/R \approx 10^5$ K, corresponds to $\Delta H_a = 198.6$ kcal mol^{-1}. For comparison, a value of 150 kcal mol^{-1} is reported by Boyer[15] for poly(bisphenol-A carbonate) which has a somewhat similar backbone to the epoxy resin used in this study. The difference in ΔH_as of ~50 kcal mol^{-1} can be accounted for by the presence of crosslinks in the epoxy resin which further restrict the mobility of the network chains. In *Figure 10*, a clear difference between dissolved and phase separated rubber is observed. Initially a large decrease of $\Delta H_a/R$ with rubber content is observed (~20% decrease at $w_R^0 = 0.05$). This is the region of dissolved rubber where samples are transparent or contain very little phase separated rubber. As the rubber content increases, part of the rubber dissolves in the matrix while the remainder phase separates. Thus, only part of the added rubber further lowers $\Delta H_a/R$ and the changes are more gradual (~40% decrease at $w_R^0 = 0.20$).

In a first approximation, the observed behaviour can be described by two straight lines, (I) and (II), whose intersection at $w_R^0 = 0.06$ marks the onset of phase separation. Line (I) represents total dissolution while line (II) represents phase separation. This value of 6% correlates well with the findings of the ΔT_g study. The slope of each line can be qualitatively interpreted as an indication of the sharpness of each stage. In the ideal case of sharp phase separation, the slope of (I) should be rather large while the slope of (II) should be small. In the ideal case of total dissolution, the two lines should blend into one continuous curve. To validate these comments, samples were moulded with a lower stoichiometric ratio, $s = 0.3$. By decreasing the relative amount of bisphenol-A, a tighter epoxy network is created. The two families of samples are compared in *Figure 11* where the ratio $\Delta H_{a_{E(r)}}/\Delta H_{a_{E(0)}}$ is plotted as a function of rubber content. $\Delta H_{a_{E(0)}}$ is the apparent enthalpy of activation for the pure epoxy. The normalization of $\Delta H_{a_{E(r)}}$ by $\Delta H_{a_{E(0)}}$ is made necessary for comparison purposes because of the slight difference

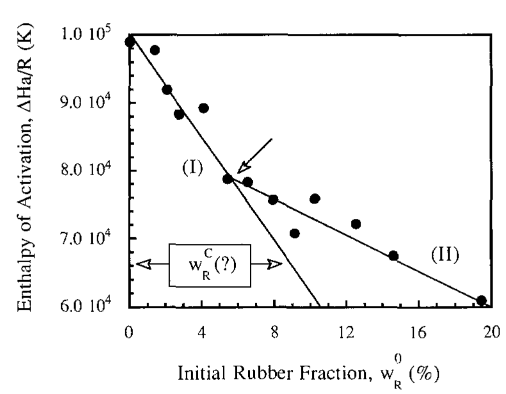

Figure 10 Apparent enthalpy of activation, $\Delta Ha_{a_{E(r)}}/R$, as a function of rubber content, w_R^0 [M/*s*/06/100 samples, (●)]. The intersection of lines (I) and (II) indicates the onset of phase separation

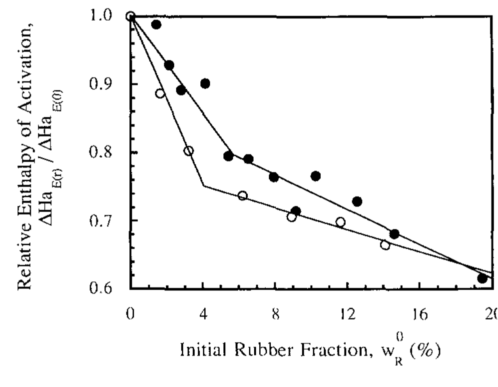

Figure 11 Effect of stoichiometry on the relative enthalpy of activation, $\Delta H_{a_{E(r)}}/\Delta H_{a(0)}$ [M/*s*06/100 samples, (●); M/*s*03/100 samples, (○)]

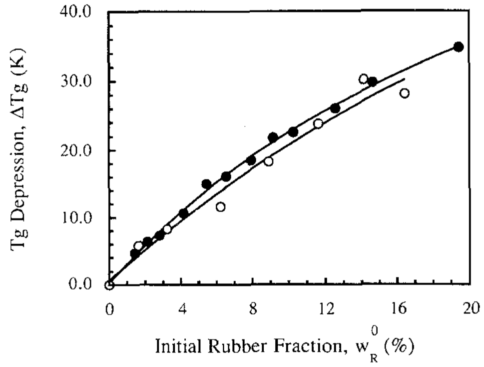

Figure 12 Effect of stoichiometry on the depression of the epoxy glass transition temperature, $\Delta T_{g_{E(r)}}$ [M/*s*06/100 samples, (●); M/*s*03/100 samples, (○)]

between $\Delta H_{a_{E(0),s03}}$ (0.91×10^5 K) and $\Delta H_{a_{E(0),s06}}$ (0.99×10^5 K). *Figure 11* shows that a tighter network decreases the amount of rubber that can be dissolved. The onset of phase separation as detected by this method now occurs at ~4% instead of 6% previously. Notice also that for M/*s*03/100 samples, the initial decrease (I) is sharper while (II) is flatter. These results indicate that $\Delta H_a/R$ is quite sensitive to the state of the rubber in the epoxy matrix. As for ΔT_g measurements, *Figure 12* shows that the drop in the T_g is less with the tighter matrix, confirming that less rubber dissolves in the continuous phase in this case.

Another important feature of the $\Delta H_a/R$ variations with rubber content is that it represents another set of data from which the amount of dissolved rubber can be evaluated. This is graphically illustrated in *Figure 10* where the dissolution stage is linearly approximated by (I). For an initial rubber content $w_R^0 = 0.15$, one finds $w_R^C(\Delta H_a/R) = 0.085$. As a confirmation, the same procedure can be used with the ΔT_g data. This yields $w_R^C(\Delta T_{g_{Fox}}) = 0.130$ and $w_R^C(\Delta T_{g_{GT}}) = 0.105$ for the same initial rubber content $w_R^0 = 0.15$. Clearly the two procedures give different results. This difference of a few percent might seem small but it cannot be ignored. Indeed, *Figure 8* indicates that the amount of rubber as small as 0.03 can decrease ΔT_g by almost 8K. Because the curve fitting of the enthalpy of activation results is empirical as opposed to that of T_g results which has a more theoretical basis, the Fox equation or Gordon–Taylor equation, $w_R^C(\Delta H_a/R)$ should be considered as an apparent determination of w_R^C, hence the added question mark in *Figure 10*. It will now be shown that the total dissolution curve should not be a straight line. For the present system, the frequency dependency of the T_g is described by an Arrhenius equation:

$$\omega = k(\mathrm{r}) \exp\left(-\frac{\Delta H_{a_{E(r)}}}{R T_{g_{E(r),\omega}}} \right) \tag{13}$$

and the composition dependency follows to a first approximation the Fox equation:

$$\frac{1}{T_{g_{E(r),\omega}}} = \frac{(1-w_R^C)}{T_{g_{E(0),\omega}}} + \frac{w_R^C}{T_{g_{R(0),\omega}}} \tag{14}$$

Equation (13) can be rewritten as:

$$\frac{1}{T_{g_{E(r),\omega}}} = -\ln\left[\frac{\omega}{k(\mathrm{r})}\right] \frac{1}{\dfrac{\Delta H_{a_{E(r)}}}{R}} \tag{15}$$

The unknown pre-exponential factor $k(\mathrm{r})$ can be eliminated by considering the change in T_g between $\omega = 1$ rad s^{-1} and a general value ω:

$$\begin{aligned} \frac{1}{T_{g_{E(r),\omega}}} - \frac{1}{T_{g_{E(r),\omega=1}}} &= -\frac{\ln\omega}{\dfrac{\Delta H_{a_{E(r)}}}{R}} \\ \frac{1}{T_{g_{R(0),\omega}}} - \frac{1}{T_{g_{R(0),\omega=1}}} &= -\frac{\ln\omega}{\dfrac{\Delta H_{a_{R(0)}}}{R}} \\ \frac{1}{T_{g_{E(0),\omega}}} - \frac{1}{T_{g_{E(0),\omega=1}}} &= -\frac{\ln\omega}{\dfrac{\Delta H_{a_{E(0)}}}{R}} \end{aligned} \tag{16}$$

From (14) and (16):

$$\begin{aligned} -\frac{\ln\omega}{\dfrac{\Delta H_{a_{E(r)}}}{R}} + \frac{1}{T_{g_{E(r),\omega=1}}} = {} & -\frac{\ln\omega}{\dfrac{\Delta H_{a_{R(0)}}}{R}} w_R^C + \frac{1}{T_{g_{R(0),\omega=1}}} w_R^C \\ & -\frac{\ln\omega}{\dfrac{\Delta H_{a_{E(0)}}}{R}} (1-w_R^C) + \frac{1}{T_{g_{E(0),\omega=1}}} (1-w_R^C) \end{aligned} \tag{17}$$

For $\omega = 1$ rad s^{-1}, equation (14) becomes:

$$\frac{1}{T_{g_{E(r),\omega=1}}} = \frac{w_R^C}{T_{g_{R(0),\omega=1}}} + \frac{(1-w_R^C)}{T_{g_{E(0),\omega=1}}} \tag{18}$$

And thus (17) yields:

$$\frac{1}{\dfrac{\Delta H_{a_{E(r)}}}{R}} = \frac{w_R^C}{\dfrac{\Delta H_{a_{R(0)}}}{R}} + \frac{(1-w_R^C)}{\dfrac{\Delta H_{a_{E(0)}}}{R}} \tag{19}$$

A similar equation can be derived assuming that the Gordon–Taylor equation is valid for the system studied. First, equation (6) needs to be rewritten as:

$$\frac{1}{T_{g_{E(r)}}} = \frac{1}{\left[(1-w_R^C) + \dfrac{k}{k_0} w_R^C\right]} \left[\frac{(1-w_R^C)}{T_{g_{E(0)}}} + \frac{\dfrac{k}{k_0} w_R^C}{T_{g_{R(0)}}}\right] \tag{20}$$

Using the same steps as before, the following equation is obtained:

$$\frac{1}{\dfrac{\Delta H_{a_{E(r)}}}{R}} = \frac{1}{\left[(1-w_R^C) + \dfrac{k}{k_0} w_R^C\right]} \left[\frac{(1-w_R^C)}{\dfrac{\Delta H_{a_{E(0)}}}{R}} + \frac{\dfrac{k}{k_0} w_R^C}{\dfrac{\Delta H_{a_{R(0)}}}{R}}\right] \tag{21}$$

Equations (19) and (21) are the analogue of the Fox equation and of the Gordon–Taylor equation for the apparent enthalpy of activation, $\Delta H_{a_{E(r)}}$. The authors are not aware of any previous derivation of equations (19) or (21). Here, the apparent enthalpy of activation for the pure epoxy, $\Delta H_{a_{E(0)}}$, and for the pure rubber, $\Delta H_{a_{R(0)}}$ are known or can be estimated (see Appendix). Thus the dissolution stage can now be correctly described by equation (21) with $k/k_0 = 1.2$. The results are shown in *Figure 13*. A more exact value of the amount of dissolved

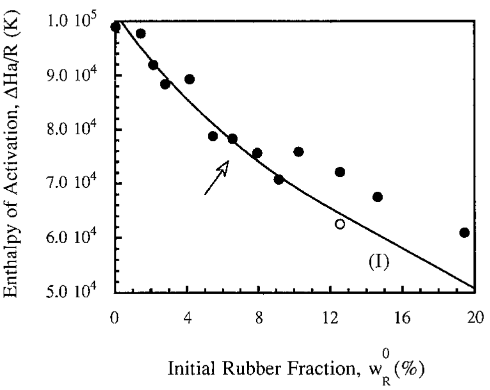

Figure 13 Apparent enthalpy of activation, $\Delta H_{a_{E(r)}}/R$, as a function of rubber content, w_R^0 [M/*s*06/100 samples, (●)]. (I) Total dissolution behaviour, as modelled by the extended Gordon–Taylor equation. (○) M/*s*06/20/150 sample

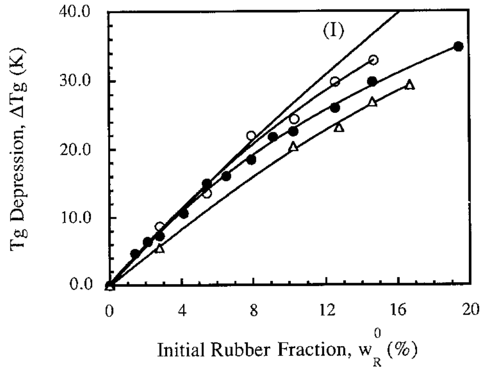

Figure 14 Effect of cure temperature on the ΔT_g depression: (△) M/*s*06/80; (●) M/*s*03/100; (○) M/*s*06/150. (I) Gordon–Taylor equation calculated for M/*s*06/150 samples only

rubber can now be determined from the enthalpy of activation measurements. At $w_R^0 = 0.15$, one finds $w_R^C(\Delta H_{a_{GT}}/R) = 0.12$ in good agreement with $w_R^C(\Delta T_{g_{GT}}) = 0.11$ obtained previously. In *Figure 13* an extra data point (○) has been included for a sample moulded at 150°C. This sample, M/*s*06/24/150, is the last one to retain some transparency at this rubber content while the corresponding M/*s*06/24/100 sample is opaque. Indeed, as shown in the next section, a higher cure temperature retards the onset of phase separation. Thus the enthalpy of activation obtained for the M/*s*06/24/150 sample can be used to help determine the value of *k* more accurately.

(2) Influence of the epoxy cure temperature. The morphology study has shown that the epoxy cure temperature has a significant effect on the amount of dispersed phase while the average particle diameter remains largely unaffected. Consequently ΔT_g is expected to be a function of the cure temperature. This is illustrated in *Figure 14* for M/*s*06/80, M/*s*06/100 and M/*s*06/150 samples. As expected, ΔT_g is reduced for $T_{cure} = 80°C$ as more rubber phase separates while larger ΔT_gs are observed for $T_{cure} = 150°C$ when most of the rubber is trapped in the continuous phase. At a given rubber content, $w_R^0 = 0.15$, the increase in T_{cure} results in higher values of w_R^C, $w_R^C(80°C) = 0.085$ *versus* $w_R^C(150°C) = 0.13$. Departure from total dissolution (as defined by the Gordon–Taylor equation) occurs in successive order, as expected. The results for the M/*s*06/150 samples can be used to confirm the previous estimate of *k*, since these samples tend to phase separate at even higher rubber content than the M/*s*06/100 samples. One finds $k_{150°C} = 2.03$, close to the $k_{100°C} = 1.95$ found earlier. Caution should also be exercised in calculating ΔT_g values for different cure conditions because the reference point, T_g of the pure epoxy, changes with T_{cure}. As an example $T_{g_{E(0)}}$ for $T_{cure} = 100°C$ is ~376 K but drops to 370K for $T_{cure} = 150°C$. Thus, in *Figure 14*, line (I) represents the Gordon–Taylor equation for samples cured at 150°C. The influence of T_{cure} on the ultimate T_g of DGEBA/bisphenol-A epoxy resins has been studied in more detail by Levita[7].

So far it has been shown that ΔT_g in the total dissolution stage can be predicted rather well by the Gordon–Taylor equation. However it would be interesting to predict in a simple way the T_g depression for samples where phase separation is significant. This can be done by assuming that the amount of rubber that dissolves into the epoxy matrix is always a constant fraction, [α], of the intial rubber content. Experimental results which seem to justify this assumption are available[4,9,20]. This assumption is reasonable for rubber contents sufficiently below the critical content for phase inversion. In this case, a generalized version of the Gordon–Taylor equation is obtained:

$$\Delta T_{g_{gen.}} = \frac{k[\alpha]w_R^0(T_{g_{E(0)}} - T_{g_{R(0)}})}{1 + [\alpha]w_R^0(k-1)} \tag{22}$$

The constant [α] depends on the rubber type, the cure temperature and the epoxy resin stoichiometric ratio (*Table 2*). The parameter [α] is obtained from the best fit of the experimental data, $\Delta T_g = f(w_R^0)$, by equation (22). The maximum error on the determination of [α] is <7%. From *Table 2*, the influence of the three parameters considered on the magnitude of the T_g drop can be ranked as followed:

rubber type > cure temperature > stoichiometric ratio

Glass transition region of the rubber. In the previous section, the overall sample has been observed from the point of view of the continuous epoxy-rich phase. It would be very interesting to gather similar information from the rubber-rich phase separated domains so that a complete picture of these systems could be obtained. However the study of the low temperature region is more complicated for several reasons. First, the intensity of the rubber glass transition is quite weak because of the low levels of rubber addition generally used. In most studies dealing with a CTBN rubber, the upper limit is ~20 wt% as a further increase in rubber content would result in phase inversion[20]. Second, if the rubber is very soluble with the epoxy matrix a significant amount of the rubber introduced just dissolves into the continuous phase and

Table 2 Influence of rubber type, stoichiometry and cure temperature on the fraction of dissolved rubber

	80°C	100°C	150°C
M/*s*06	0.67 ± 0.01	0.77 ± 0.025	0.92 ± 0.02
M/*s*03		0.73 ± 0.05	
L/*s*06		0.43 ± 0.01	

a very weak glass transition for the dispersed phase is observed. Third, the glass transition of the rubber most commonly used (i.e. polybutadiene based) often overlaps with a broad β relaxation of the epoxy resin associated with the movement of hydroxyether units. It then becomes difficult to observe the glass transition of the rubber at low rubber content unless very low test frequencies are used to separate the two transitions. Also, whereas the continuous phase is truly homogeneous, this does not always seem to be the case for the dispersed phase. Core–shell morphologies[21] as well as the presence of epoxy phase separated regions[22] inside rubber-rich dispersed domains have been reported. Last, and perhaps most interesting, is the fact that several authors have reported[23] that the T_g of the dispersed domains is close to or in some cases *less* than that of the pure rubber. If anything, one would expect T_g to increase because of the presence of slow moving epoxy monomers or oligomers inside the rubber domains. These results were explained in terms of the presence of interfacial stresses (tension) due to the difference in thermal expansion coefficients between the epoxy matrix and the rubber domains[24]. This stress induced depression, $\Delta T_{g_{\mathrm{stress}}}$, is usually small and of the order of 5K. However small, this shift of the true T_g is enough to prohibit an analysis of the results in terms of the Gordon–Taylor equation. Indeed if $\Delta T_{g_{\mathrm{stress}}}$ brings the T_g of the dispersed phase below that of the pure rubber, the Gordon–Taylor equation ceases to be meaningful.

Figure 15 shows the effect of cure temperature on the shape of the tan δ spectrum in the low temperature region. Here T_g is defined as the temperature for which the loss factor tan δ is maximum, as this maximum is usually more distinct in the tan δ spectrum than in the G'' spectrum. In *Figure 15*, a low frequency of 0.1 rad s^{-1} has been used to separate the relaxation of the rubber domains (centred at $-53°C$) from the broad epoxy β relaxation (centred at $-92°C$). Low frequencies are helpful here only because the enthalpy of activation of the epoxy β relaxation is about four times smaller than that associated with the rubber relaxation ($\Delta H_a/R \cong 10^4$ K *versus* 4×10^4 K). As mentioned earlier, the T_g of the rubber domains is observed at lower temperature ($\sim -49°C$ at 1 rad s^{-1}; *Figure 7*) than that for the pure rubber. Thus equation (7) cannot be used to determine the amount of epoxy dissolved in the dispersed phase. However the enthalpy of activation associated with the relaxation of the rubber domains is larger than that for the pure rubber, i.e. $\Delta H_{a_{R(e)}} > \Delta H_{a_{R(0)}}$, even though the trend is reversed with the T_g, i.e. $T_{g_{R(e)}} < T_{g_{R(0)}}$. The opposite would be expected if the presence of epoxy oligomers in the phase separated domains had no influence on $\Delta H_{a_{R(e)}}$ because ΔH_a is known to decrease continuously with decreasing T_g (see, for example, the review by Boyer[15]). Thus it is suggested that the extended Gordon–Taylor equation may be used to determine directly the composition of the dispersed phase from the increase in $\Delta H_{a_{R(e)}}$.

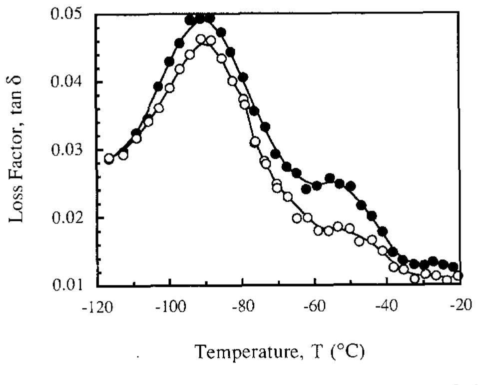

Figure 15 Influence of cure temperature on the shape of the tan δ spectrum in the rubber glass transition region: (○) M/s06/24/150; (●) M/s06/24/80

Figure 15 also shows that the area under the glass transition of the rubber peak is larger for a sample cured at lower temperature. This is consistent with the results of the SEM study which show that the volume fraction of dispersed phase is larger in this case (*Figures 5* and *6*) and with the results of the ΔT_g study which show that the amount of rubber lost to the continuous phase is lower at a lower cure temperature. This trend between the area and the volume fraction can be rationalized using Kramers–Kronig analysis[12].

CONCLUSIONS

Blends of hydroxyl terminated, internally epoxidized polybutadiene rubber and epoxy resin have been characterized by SEM and d.m.a. The influence of parameters such as rubber content, rubber type, stoichiometry, and cure cycle on the physical properties and morphology of these blends was established.

It was first shown that the T_g of the epoxy-rich continuous phase depends heavily on the amount of dissolved rubber. This behaviour can be modelled using the Gordon–Taylor equation which was found to describe the present system much more accurately than the more commonly used Fox equation. It was further shown that the apparent enthalpy of activation associated with the glass transition also strongly depends on the amount of dissolved rubber. The Gordon–Taylor equation can be extended in a simple manner to describe this behaviour. Finally, the Gordon–Taylor equation was generalized to predict the T_g for a sample containing both dissolved and phase separated rubber.

On the other hand, the study of the glass transition region of the rubber-rich dispersed phase is more difficult because this transition overlaps with the broad β relaxation of the epoxy resin. The intensity of the rubber relaxation is weak when a medium-epoxidized rubber is used, consistent with the fact that there is little phase separation in this case. The area under the rubber peak also correlates with the cure temperature.

ACKNOWLEDGEMENT

Financial support from Elf-Atochem during the course of this study is gratefully acknowledged.

REFERENCES

1 Riew, C. K., Rowe, E. H. and Siebert, A. R. *Adv. Chem. Ser.* 1976, **154**, 326
2 Pearson, R. A. and Yee, A. F. *J. Mater. Sci.* 1986, **21**, 2462
3 Kinloch, A. J. *Adv. Chem. Ser.* 1989, **222**, 67
4 Bussi, P. and Ishida, H. *J. Polym. Sci., Polym. Phys. Edn* in press
5 Ishida, H. and Smith, M. E. *Rheol. Acta* 1991, **30**, 184
6 Levita, G., Marchetti, A., Lazzeri, A. and Frosini, V. *Polym. Comp.* 1987, **8**, 14
7 Levita, G. *Adv. Chem. Ser.* 1989, **222**, 93
8 Bussi, P. and Ishida, H. *J. Appl. Polym. Sci.* submitted

9 Verchere, D., Pascault, J. P., Sautereau, H., Moschiar, S. M., Riccardi, C. C. and Williams, R. J. J. *J. Appl. Polym. Sci.* 1991, **42**, 701
10 Butta, E., Levita, G., Marchetti, A. and Lazzeri, A. *Polym. Eng. Sci.* 1986, **26**, 63
11 Williams, R. J. J., Borrajo, J., Addabo, H. E. and Rojas, A. J. *Adv. Chem. Ser.* 1984, **208**, 195
12 Bussi, P. and Ishida, H. *Macromolecules* submitted
13 Fox, T. G. *Bull. Am. Phys. Soc.* 1956, **1**, 123
14 Gordon, M. and Taylor, J. S. *J. Appl. Chem.* 1952, **2**, 493
15 Boyer, R. F. in 'Encyclopedia of Polymer Science and Technology' (Eds H. F. Mark *et al.*), Supplement Vol. II, Wiley, New York, 1977, p. 745
16 Kaelble, D. H. in 'Epoxy Resins: Chemistry and Technology' (Eds C. A. May and Y. Tanaka), Marcel Dekker, New York, 1973, p. 346
17 Boyer, R. F. *Polym. Eng. Sci.* 1968, **8**, 161
18 Kinloch, A. J. and Hunston, D. L. *J. Mater. Sci. Lett.* 1987, **6**, 137
19 Williams, M. L., Landel, R. F. and Ferry, J. D. *J. Am. Chem. Soc.* 1955, **77**, 3701
20 Verchere, D., Sautereau, H., Pascault, J. P., Moschiar, S. M., Riccardi, C. C. and Williams, R. J. J. *J. Appl. Polym. Sci.* 1990, **41**, 467
21 Romanchik, W. A., Sohn, J. E. and Geibel, J. F. *Adv. Chem. Ser.* 1983, **221**, 85
22 Pearson, R. A. and Yee, A. F. *J. Mater. Sci.* 1986, **21**, 2475
23 Manzione, L. T., Gillham, J. K. and McPherson, C. A. *J. Appl. Polym. Sci.* 1981, **26**, 889
24 Beck, R. H., Gratch, S., Newman, S. and Rusch, K. C. *Polym. Lett.* 1968, **6**, 707
25 Lewis, O. G. and Gillham, J. K. *J. Appl. Polym. Sci.* 1963, **7**, 685
26 Stephens, H. L. in 'Polymer Handbook' (Eds J. Brandrup and E. H. Immergut), Wiley, New York, 1989, p. V/I
27 Boyer, R. F. *J. Macromol. Sci.* 1974, **B9**, 187

APPENDIX

In order to apply the Gordon–Taylor equation or the Fox equation and their extended version, the T_g and the enthalpy of activation for the epoxidized rubber must be known. Moreover, these quantities have to be determined by d.m.a., at 1 rad s^{-1}, to be consistent with the rest of the experimental data. Unfortunately, the instrument is not truly equipped to measure the glass transition of low molecular weight, low viscosity liquids, because of the limited sensitivity of the transducer to this type of samples. Rather, torsional braid analysis (TBA), developed by Lewis and Gillham[25], is used in such cases. In order to alleviate this problem, rectangular torsion samples containing 40 wt% of glass beads were moulded between aluminium foils. The glass beads were added to increase the viscosity of the epoxidized rubber. The composite sample is then immersed in liquid nitrogen and is later mounted quickly in the d.m.a. instrument, which has been equilibrated in advance at −125°C. A frequency/temperature sweep is then performed up to the temperature at which the sample collapses in the fixtures. *Figure A1* shows that this collapse occurs immediately after the maximum in the relative loss modulus is observed. Thus the T_g can be obtained, $T_g = -60$°C for the low-epoxidized rubber and $T_g = -47$°C for the medium-epoxidized rubber. The T_g for the non-epoxidized rubber can be obtained from the literature and from the knowledge of the microstructure. Indeed, high vinyl content polybutadiene has a substantially higher T_g (−15°C) than either high *cis* content polybutadiene ($T_g = -95$°C) or high *trans* content polybutadiene ($T_g = -83$°C)[26]. Thus T_g of the non-epoxidized rubber was determined from the Fox equation, using the distribution of unsaturations determined elsewhere[8]. This procedure yields a T_g of −75°C. Boyer[27] reports a value of −79°C, as measured by TBA for an emulsion polybutadiene containing 55% *trans* units.

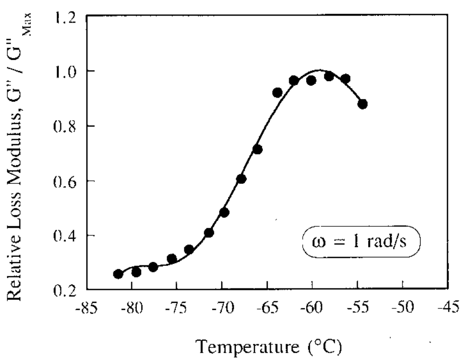

Figure A1 Determination of the glass transition temperature, T_g, of the low-epoxidized rubber ($T_g \cong -60$°C)

The determination of the apparent enthalpy of activation is more difficult since the presence of glass beads is likely to affect the value of $\Delta H_a/R$. Moreover the sample generally collapses in the fixtures before the glass transition can be observed at higher frequencies. Nonetheless an estimated experimental upper-bound value, $\Delta H_a/R < 0.25 \times 10^5$ K, could be obtained. As a lower-bound value of $\Delta H_a/R$, one can use the value quoted by Boyer[15] for Hevea rubber (natural rubber), which has a somewhat similar structure and glass transition temperature, $T_g = -73$°C, to polybutadiene. Boyer reports $\Delta H_a/R = 0.15 \times 10^5$ K.

Ultimately, $\Delta H_a/R$ for the medium-epoxidized rubber can be determined directly from the experimental data shown in *Figure 13*. The enthalpy of activation is obtained as the best fit of the extended Gordon–Taylor equation for optically clear samples, while fixing the value of the parameter k at two, as determined in the ΔT_g study. From the two sets of data, samples moulded at 100°C and samples moulded at 150°C, an average value, $\Delta H_a/R = 0.20 \times 10^5$ K, could be obtained for the medium-epoxidized rubber.